Cooling a Harmonic Oscillator by Optomechanical Modification of Its Bath

Xunnong Xu, Thomas Purdy, and Jacob M. Taylor

Phys. Rev. Lett. **118**, 223602 — Published 31 May 2017

DOI: 10.1103/PhysRevLett.118.223602

Cooling a harmonic oscillator by optomechanical modification of its bath

Xunnong Xu,[1] Thomas Purdy,[1] and Jacob M. Taylor[1, 2]

[1] *Joint Quantum Institute, University of Maryland/National Institute of Standards and Technology, College Park, Maryland 20742, USA*

[2] *Joint Center for Quantum Information and Computer Science, University of Maryland, College Park, Maryland 20742, USA*

(Dated: May 2, 2017)

Optomechanical systems show tremendous promise for high sensitivity sensing of forces and modification of mechanical properties via light. For example, similar to neutral atoms and trapped ions, laser cooling of mechanical motion by radiation pressure can take single mechanical modes to their ground state. Conventional optomechanical cooling is able to introduce additional damping channel to mechanical motion, while keeping its thermal noise at the same level, and as a consequence, the effective temperature of the mechanical mode is lowered. However, the ratio of temperature to quality factor remains roughly constant, preventing dramatic advances in quantum sensing using this approach. Here we propose an approach for simultaneously reducing the thermal load on a mechanical resonator while improving its quality factor. In essence, we use the optical interaction to dynamically modify the dominant damping mechanism, providing an optomechanically-induced effect analogous to a phononic band gap. The mechanical mode of interest is assumed to be weakly coupled to its heat bath but strongly coupled to a second mechanical mode, which is cooled by radiation pressure coupling to a red detuned cavity field. We also identify a realistic optomechanical design that has the potential to realize this novel cooling scheme.

PACS numbers: 42.50.Wk, 07.10.Cm, 42.50.Lc, 42.50.Dv

Recent years have seen dramatic experimental and theoretical progress in optomechanics [1, 2], ranging from ground state cooling [3] and squeezing [4, 5] to quantum nonlinear optomechanics [6–11]. These advances rely upon improvements in optomechanical coupling, particularly the single phonon-single photon coupling rate, and upon increasing mechanical quality factor, which enables lower heat loads and corresponds to higher sensitivity and longer quantum coherence times. However, the longer-term target of single photon nonlinear optics with optomechanical systems remains out of reach. Furthermore, for many sensing applications, the thermal noise remains a fundamental limit for relevant resonator designs, regardless of progress in the use of quantum correlations [4, 5, 12], as typically the signal to be sensed is transduced to a force on the mechanical system which is in competition with the quantum Brownian motion-induced Langevin force from the thermal bath.

In the present work, we shall focus on thermal noise reduction for mechanical resonators, utilizing the standard tool box provided by optomechanics. This is crucial for improving the signal-to-noise ratio of mechanical devices, operating either in the classical regime or in the quantum regime. We are motivated by recent advances in phononic-band gap engineering as a principle for improved quality factor [13–15] – but here, we engineer a dissipative band-gap dynamically via the optomechanical interaction, rather than a constant bandgap during fabrication. Specifically, we introduce a generic coupled-oscillator model to describe mechanical systems whose damping is primarily via elastic wave radiation through the boundary, i.e., clamping loss. We then consider how optomechanical coupling to the clamping region enables dynamical control over the coupled mechanical resonator. This leads to the counterintuitive outcome: increasing optical power simultaneously reduces the temperature and linewidth of the mechanical mode, in contrast to direct optomechanical cooling. After introducing this model, we describe a specific resonator design that enables testing of these concepts using current techniques, and analyze the regime in which clamping losses are likely to dominate, finding that at low temperature and high mechanical frequencies our approach may find wide application.

This idea of cooling a mechanical oscillator indirectly via its coupling to another oscillator, sympathetic cooling, has been demonstrated in dual species ions in an ion trap [16], in the production of two overlapping Bose-Einstein Condensates [17], and recently in SiN membrane coupled to an atomic ensemble [18]. The use of optomechanical interactions to modify an oscillator's bath has also been discussed in [19], in a different setup. An important advantage of our approach is that ground state sympathetic cooling can be achieved with a simultaneous linewidth reduction. This provides an in situ means of improving the quantum coherence time for devices that start with substantial clamping losses. For protocols [20] that require starting in the ground state and also require a large quantum coherence time, our approach allows continuous cooling of the system.

Toy model– We consider a toy model of two coupled quantum harmonic oscillators with annihilation operators a and b, resonant frequencies ω_a and ω_b, and a coupling strength between them λ. Each harmonic oscillator is also coupled to its own heat bath at temperature T_a and T_b with rates γ_a and γ_b. In addition, optomechanical cooling is introduced to oscillator b via coupling to a red detuned optical mode c with frequency ω_c and damping κ, as shown in Fig. (1).

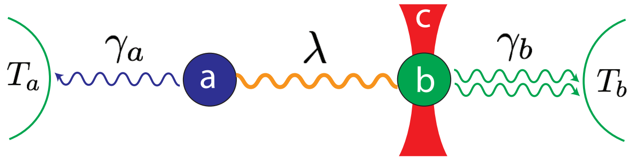

FIG. 1. (color online). Schematic of the coupled harmonic oscillator system, with optomechanical cooling on oscillator b. We are interested in the regime where a couples weakly to its heat bath, which means $\gamma_a \ll \lambda, \gamma_b$.

The effective Hamiltonian of the three mode system when pumped with a laser follows immediately (with $\hbar = 1$, and neglecting the weak nonlinear correction):

$$\begin{aligned} H_{\text{eff}} = &-\Delta c^\dagger c + \omega_a a^\dagger a + \omega_b b^\dagger b + \lambda(a + a^\dagger)(b + b^\dagger) \\ &-\alpha g_0 (b + b^\dagger)(c + c^\dagger). \end{aligned} \tag{1}$$

where $\alpha = E/(i\Delta - \kappa/2)$ is the pump-induced coherent state in the optical cavity and assumed to be real without loss of generality (by choosing an appropriate phase for the pump strength E), g_0 is the quantum optomechanical coupling, and $\Delta = \omega_p - \omega_c$ is the detuning of the pump laser. We consider $\omega_a \sim \omega_b \sim -\Delta$, and include mechanical damping of a and b with rates γ_a, γ_b, and optical loss with rate κ [2]. Under the rotating wave approximation, the Heisenberg-Langevin equations in the input-output formalism are as follows:

$$\dot{c} = i\Delta c - \frac{\kappa}{2} c + i\alpha g_0 b + \sqrt{\kappa} c_{\text{in}}, \tag{2a}$$

$$\dot{a} = -i\omega_a a - \frac{\gamma_a}{2} a - i\lambda b + \sqrt{\gamma_a} a_{\text{in}}, \tag{2b}$$

$$\dot{b} = -i\omega_b b - \frac{\gamma_b}{2} b - i\lambda a + i\alpha g_0 c + \sqrt{\gamma_b} b_{\text{in}}. \tag{2c}$$

This set of linear equations can be solved by moving to the frequency domain. We successively solve for c, then b, then a. For example, $c = \frac{i\alpha g_0 b + \sqrt{\kappa} c_{\text{in}}}{-i(\omega+\Delta)+\kappa/2}$. We immediately set $c \approx \frac{1}{\alpha g_0}(i\frac{\Gamma}{2} b + \sqrt{\Gamma} c_{\text{in}})$ in the sideband-resolved limit with $|\Delta + \omega| \ll \kappa/2$ where $\Gamma = 4|\alpha g_0|^2/\kappa$ is the optically-induced damping of mode b. This makes sure that we are only looking at a narrow range of frequency within the cavity linewidth, so that we can solve c easily. Continuing, we find

$$\chi_b^{-1} b = -i\lambda a + \sqrt{\gamma_b} b_{\text{in}} + i\sqrt{\Gamma} c_{\text{in}} \tag{3a}$$

$$\text{where } \chi_b = [-i(\omega - \omega_b) + (\gamma_b + \Gamma)/2]^{-1} \tag{3b}$$

is the susceptibility of mode b for $\lambda = 0$.

Finally, we find for mode a

$$\chi_a^{-1} a = \sqrt{\gamma_a} a_{\text{in}} - i\chi_b \lambda \left(\sqrt{\gamma_b} b_{\text{in}} + i\sqrt{\Gamma} c_{\text{in}} \right) \tag{4a}$$

$$\text{with } \chi_a = \left[-i(\omega - \omega_a) + \gamma_a/2 + \chi_b \lambda^2 \right]^{-1} \tag{4b}$$

Examining these equations, we see that mode a's resonant response, as described by the susceptibility χ_a, have a frequency and damping that depend, via $\lambda^2 \chi_b$, upon the properties of the optomechanically damped mode b. Specifically, examining the real and imaginary components, we have

$$\omega_a' = \omega_a + \frac{\lambda^2(\omega - \omega_b)}{(\omega - \omega_b)^2 + (\gamma_b + \Gamma)^2/4}, \tag{5a}$$

$$\gamma_a' = \gamma_a + \frac{\lambda^2(\gamma_b + \Gamma)}{(\omega - \omega_b)^2 + (\gamma_b + \Gamma)^2/4}, \tag{5b}$$

Let us examine the particular scenario when the cooperativity between a and b satisfies $\mathcal{C}_{ab} \equiv \frac{4\lambda^2}{\gamma_a \gamma_b} \gg 1$ and $\frac{\gamma_b + \Gamma}{\gamma_a} \gg \mathcal{C}_{ab}$. This corresponds to the intrinsic damping of mode a being dominated by its coupling through b to b's bath, while simultaneously being able to examine b's response as broader than a's. We will further focus on $|\omega_b - \omega_a| \ll \gamma_b + \Gamma$, as provides the maximum modification of damping. This allows us to expand $\omega_a' \approx \omega_a$ and $\gamma_a' \approx \gamma_a + \Gamma_a$ with $\Gamma_a \equiv \frac{4\lambda^2}{\gamma_b + \Gamma}$. When the optomechanical damping of mode b increases, the linewidth of mode a becomes narrower, and eventually reaches its intrinsic damping γ_a. We finally get

$$a \approx \frac{\sqrt{\gamma_a} a_{\text{in}} + i\sqrt{\Gamma_a \left(\frac{\gamma_b}{\gamma_b + \Gamma} \right)} b_{\text{in}} + \sqrt{\Gamma_a \left(\frac{\Gamma}{\gamma_b + \Gamma} \right)} c_{\text{in}}}{-i(\omega - \omega_a) + (\gamma_a + \Gamma_a)/2} \tag{6}$$

This regime (damping of a primarily via mode b, which in turn is damped optically by a sideband-resolved coupling to mode c) lets us examine the effective temperature. Specifically, using the input noise correlations of b_{in} in the frequency domain,

$$\left\langle b_{\text{in}}^\dagger(\omega) b_{\text{in}}(\omega') \right\rangle = \bar{n} \delta(\omega + \omega') \tag{7a}$$

$$\left\langle b_{\text{in}}(\omega) b_{\text{in}}^\dagger(\omega') \right\rangle = (\bar{n} + 1) \delta(\omega + \omega') \tag{7b}$$

where $\bar{n} = 1/(e^{\hbar\omega/k_B T} - 1)$ is the average phonon occupation number of a harmonic oscillator of frequency ω when it is in thermal equilibrium with a heat bath at temperature T. We have the same for a_{in} and c_{in}, and we assume $T_a = T_b = T_c = T$. The optical frequency is many orders of magnitude higher than mechanical frequency, so at the same temperature, the photon occupation number of the optical environment is completely negligible. When the two mechanical frequencies are large and close to each other, it is reasonable to neglect the possible squeezing terms, so we can find the average position fluctuation by $n_{\text{eff}} + 1/2 \equiv \left\langle (a + a^\dagger)^2 \right\rangle /2$ (since $\langle n | (a + a^\dagger)^2 | n \rangle = 2n + 1$) to be

$$n_{\text{eff}} = \frac{\gamma_a \bar{n} + \Gamma_a \left(\frac{\gamma_b}{\Gamma + \gamma_b} \bar{n} \right)}{\gamma_a + \Gamma_a} \tag{8}$$

where $\bar{n}$ is evaluated at ω_a. This expression is also consistent with the result from detailed balance relation [21].

We can minimize this occupation by a setting the optomechanical cooperativity $\mathcal{C}_{\text{OM}} \equiv \Gamma/\gamma_b$ of b to

$$\mathcal{C}_{\text{OM}} \to \mathcal{C}_{\text{OM}}^* \equiv \sqrt{1+\mathcal{C}_{ab}} \ ,$$

which gives

$$\frac{n_{\text{eff}}^*}{\bar{n}} = \frac{2}{1+\sqrt{1+\mathcal{C}_{ab}}}.$$

Thus in principle even ground state cooling is achievable, if the mechanical oscillator cooperativity $\mathcal{C}_{ab} \gtrsim 16\bar{n}^2$. Curiously, this cooling arises with a reduction of the linewidth of mode a, with the linewidth at the optimum power set by $\gamma_a + \Gamma_a^* = \gamma_a\sqrt{1+\mathcal{C}_{ab}}$, which is still more than the intrinsic damping.

Finally, to confirm these approximations, we numerically examine the same regime, but without making the rotating wave approximation or any narrowband approximations – this enables us to include counter-rotating terms and their associated heating. We plot the rescaled position fluctuation spectrum $S_{xx}(\omega) = \int_{-\infty}^{+\infty} \mathrm{d}t e^{i\omega t} \langle x(t)x(0)\rangle$ and rescaled effective temperature T_{eff}/T below in Fig. (2). We find that when $g_0\alpha, \lambda \ll \omega_a, \omega_b$ our approximate theory and the exact results are in agreement.

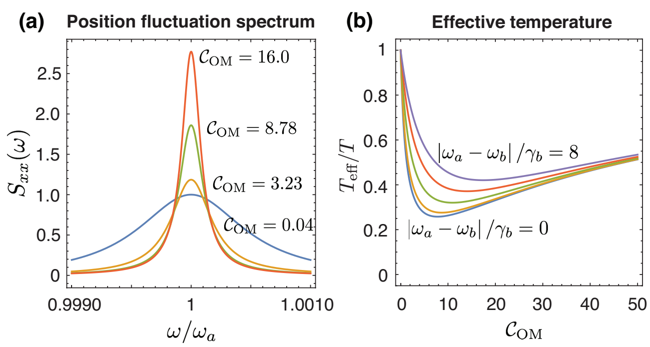

FIG. 2. (color online). (a) Rescaled position fluctuation spectrum for different values of optomechanical cooperativity $\mathcal{C}_{\text{OM}}$, with the mechanical oscillator cooperativity chosen as $\mathcal{C}_{\text{ab}} = 8$; (b) Rescaled effective temperature as a function of $\mathcal{C}_{\text{OM}}$ for $\mathcal{C}_{\text{ab}} = 50$ and different values of $|(\omega_a - \omega_b)|/\gamma_b$.

Example implementation– To design an optomechanical system that captures the main features of the toy model, we need three basic components: i) two coupled mechanical resonators; ii) one resonator is limited by thermoelastic damping, and the other is limited by clamping loss; iii) optomechanical cooling primarily on the second resonator. With these goals in mind, an example design is shown in Fig. (3). We use two nearly identical quarter- wave mechanical resonators on the left arm and right arm of a large beam resonator, denoted as a_L and a_R, to form a tuning-fork resonator as is commonly used in atomic force microscopy (AFM). To complete the analogy, we include an AFM tip in the design.

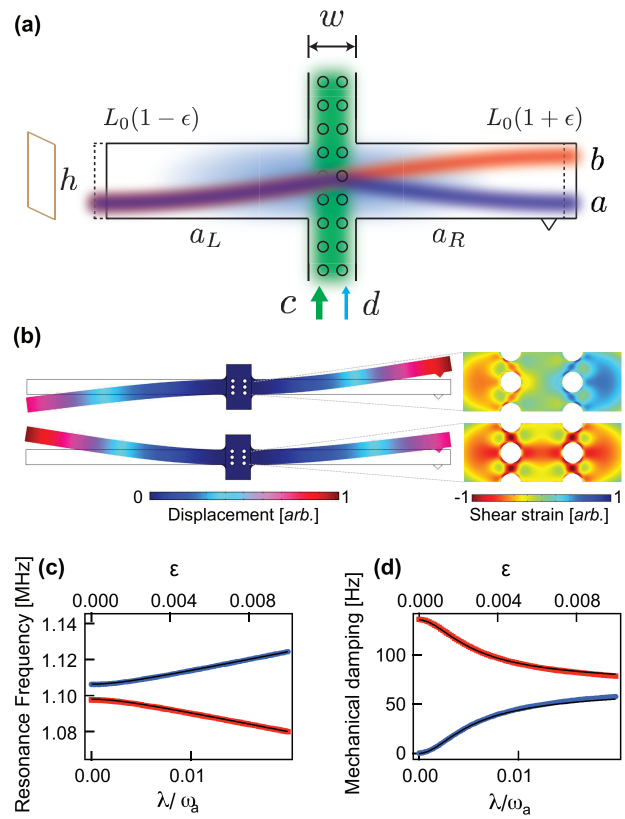

FIG. 3. (color online). (a) Optomechanical design consisting of two similar quarter-wave beam resonators, nominal length L_0, coupled through a center support region, width w, containing a photonic crystal optical structure that supports two optical modes c and d. (b) Simulated symmetric (top) and antisymmetric (bottom) eigenmodes, $\epsilon \approx 0$. Insets show the strain deformation of a single photonic defect (envisioned as part of a "zipper" photonic crystal resonator) that would lead to a strong strain-induced optomechanical coupling only between optical and mechanical modes of the same parity. (c,d) As the asymmetry, ϵ, is increased, the antisymmetric and symmetric modes are increasingly coupled, shifting the simulated eigenfrequencies and clamping losses (red squares, blue circles), consistent with fits to the theoretical model of Eq. (1) (black). Simulation parameters are L_0=20 μm, h=0.3 μm, and w = 0.5 μm, corresponding to $\omega_0 = 2\pi \times 1.102$ MHz and $\gamma_b/2 = 2\pi \times 70$ Hz clamping loss for an individual arm fabricated from silicon nitride.

To examine the mode structure, we consider coupling between the left and right sides through the support structure with a strength J. We see that symmetrical coupling of a_L and a_R through the support leads to normal modes $a = 1/\sqrt{2}(a_L + a_R)$ and $b = 1/\sqrt{2}(a_L - a_R)$, with the former having no clamping loss for $\epsilon = 0$ and the latter a clamping loss $\gamma_b \approx J^2\rho$ (by Fermi's golden rule). Physically, the symmetric mode has destructive interference which prevents excitation of support structure and the associated clamping loss, analogous to the reduction in damping observed in tuning-fork resonators, which can be seen in Fig. (3d) below.

Unfortunately, the left and right elements are not completely symmetric. This can be because of the difference in loaded mass between the two arms due, e.g., to the tip structure, though recent results suggest this can be corrected for by careful fabrication [22]. The other effect is unavoidable in AFM: the gradient of the force felt by the tip leads to an additional spring-like restoring force to the tip arm resonator a_L, and a shift in the resonance frequency. Indeed, in non-contact AFM (nc-AFM) this effect can be substantially larger than the linewidths [22–24]. These asymmetries leads to different resonant frequencies for the two resonators in the left-right basis, with $\omega_L = \omega_0(1+\epsilon)$ and $\omega_R = \omega_0(1-\epsilon)$, as shown in Fig. (3). Using the tuning fork eigenmode basis, we have asymmetry coupling a and b together with a rate $\lambda = \epsilon\omega_0$.

For readout in our proposed structure, we introduce a "zipper" photonic crystal cavity system where optical modes c and d are the anti-bond and bond fundamental [25] in the center of the beam (the support structure), with odd and even parity respectively. As shown in the simulation in Fig. (3b), the anti-bond optical mode c couples mostly to the anti-symmetric mechanical mode b, while the bond optical mode d couples mostly to the symmetric mechanical mode a. Experimentally, mode c can be driven strongly to achieve the desired optomechanical cooling, and mode d serves as a weak probe in order to make measurements on mode a.

As the toy model suggests, the damping of oscillator a is assumed very weak ($\gamma_a \ll \gamma_b, \lambda$), so that the optomechanical cooling of oscillator b could be effectively "exported" to a through phonon tunneling. This naturally leads us to the question: what kind of oscillator design has this property? There are two main sources of mechanical damping in micro- and nano-mechanical resonators [26]: i) Boundary damping, or clamping loss, e.g elastic wave radiation from the material to its base through the boundary, and ii) material damping, which includes thermoelastic damping (TED), phonon-phonon interactions. The clamping loss represents the coupling from a resonator to its base, since phonons are exchanged through the boundary, while thermoelastic damping is the major contribution to the internal damping rate of a resonator.

Clamping loss has been studied extensively in the literature [27–30]. For a beam resonator where the thickness of the beam resonator is much smaller than the wavelength of the elastic wave propagating in its support, the flexural vibration can be described using the ideal beam theory. The support of clamping-free (C-F) beam resonators is usually modeled as semi-infinite and infinite thin-plate, respectively, with the same thickness as the beam resonator; all the vibration energy of a beam resonator entering the support structure is considered to be lost. It is the vibrating shear force that induces this energy loss. In [28], they studied the clamping loss using elastic wave radiation theory and found the quality factor of clamping-free (C-F) beam resonators to be:

$$Q_{\mathrm{C-F}} \propto (L/h)^2 \tag{9}$$

where L is the length of the beam and h is its width.

Secondly, we look at the thermoelastic damping [31, 32]. Phonons traveling through a large elastic material will experience damping due to their nonlinear interaction with a surrounding bath of phonons. In the diffusive regime where the mean free path of these thermal phonons is much smaller than the wavelength of the acoustic mode, the interaction between the phonon mode and the thermal bath is captured by the material's thermal expansion coefficient (TEC), defined as $\alpha \equiv \frac{1}{L}\frac{\partial L}{\partial T}$, which is temperature dependent. According to [33], the quality factor corresponding to this damping mechanism is given by

$$Q_{\mathrm{TED}}^{-1} = \frac{E\alpha^2 T}{C_p} f(h/h_0), \tag{10}$$

where E is the material's Young's modulus, T is the temperature, C_p is the heat capacity at constant pressure, and $f(h/h_0)$ is a beam geometry function parametrized by a critical beam width h_0.

A detailed numerical estimate of these losses for a specific mechanical resonator such as SiN is possible, but here we remark that for short beams, the clamping loss, which grows as h^2/L^2, will always tend to dominate over the thermoelastic damping. For example, for a resonator with frequency $\Omega/2\pi = 1$ MHz, we have $h_0 = 6.546\ mm$. When $h \ll h_0$, we find $f(h/h_0) \to 5h^2/h_0^2$, which gives us a very high Q_{TED} (well beyond the usual material limits).

Analysis of force sensing– The proposed scheme for reducing the thermal load of the mechanical oscillator is useful for force sensing, where thermal noise is a main obstacle towards building ultra-sensitive force detection devices. In our proposed structure Fig. (3b), the mechanical mode of interest a couples to anti-bonded weak probe mode d, which has different parity from the bonded strong pump mode c and also higher frequency. Measuring the optical output signal $S(\omega)$ from d allows the sensing of force $f(\omega)$ experienced by mechanical mode a, as shown in [12]:

$$S(\omega) = \chi_X X_{d,\mathrm{in}}(\omega) + \chi_Y Y_{d,\mathrm{in}}(\omega) + \chi_F[F_{\mathrm{in}}(\omega) + f(\omega)], \tag{11}$$

with X, Y the quadratures of optical field and χ the susceptibilities for optical and force inputs.

We find that there exist a simple relation between the ultimate sensitivity (in units of $N/\sqrt{\mathrm{Hz}}$) for a mechanics based device and its thermal noise level, which can be calculated as the power spectral density of thermal fluctuating forces:

$$\eta(\omega) \equiv \sqrt{S_{FF}(\omega)} = \sqrt{\int_{-\infty}^{+\infty} \mathrm{d}t e^{i\omega t} \langle F_{\mathrm{in}}(t) F_{\mathrm{in}}(0)\rangle} \tag{12}$$

In the case of our coupled harmonic oscillator system, if oscillator a is used for force sensing, then we get better sensitivity because of the reduction in its thermal load. The force on a harmonic oscillator is defined as

$$F = \dot{p} = -i\sqrt{\frac{\hbar m\omega_a}{2}}(\dot{a} - \dot{a}^{\dagger}), \tag{13}$$

so the corresponding fluctuating force in frequency domain can be found from Eq. (6)

$$F_{\rm in}(\omega) = -i\sqrt{\frac{\hbar m\omega_a}{2}}\left[\sqrt{\gamma_a}a_{\rm in} + i\sqrt{\Gamma_a\left(\frac{\gamma_b}{\gamma_b+\Gamma}\right)}b_{\rm in} - \text{h.c.}\right] \tag{14}$$

Using the noise correlation functions Eq. (7), we can calculate its spectral density in the narrow band limit as

$$\begin{aligned} S_{FF}(\omega) &= \int d\omega' \left\langle |F_{\rm in}(\omega)F_{\rm in}(\omega')|\right\rangle \\ &= \frac{\hbar m\omega_a}{2}\left[\gamma_a + \Gamma_a\left(\frac{\gamma_b}{\gamma_b+\Gamma}\right)\right](2\bar{n}+1) \\ &\approx m\left[\gamma_a + \frac{4\lambda^2\gamma_b}{(\gamma_b+\Gamma)^2}\right]k_{\rm B}T \\ &= \left[1 + \frac{\mathcal{C}_{ab}}{(1+\mathcal{C}_{\rm OM})^2}\right]m\gamma_a k_{\rm B}T \end{aligned} \tag{15}$$

where we recall $\mathcal{C}_{\rm OM} = \Gamma/\gamma_b$ is the optomechanical cooperativity and $\mathcal{C}_{ab} = \frac{4\lambda^2}{\gamma_a\gamma_b}$ is the cooperativity between a and b. When the optically induced damping rate Γ is large compared to γ_b, we have substantial noise reduction and thus improved sensitivity for the device compared to conventional optomechanical cooling. In the latter case, we could have the noise floor of Eq. (15) but with $\mathcal{C}_{\rm OM} = 0$.

Summary– Here we proposed an efficient scheme for cooling a harmonic oscillator by decreasing dissipation via optomechanical cooling. We studied the practical conditions to realize this cooling scheme, and also identified a realistic optomechanical design that has the potential to realize it. Potential applications include mechanics based force sensing, and other related areas where reducing the thermal load via non-conventional techniques is needed. some of the quantum communication and transduction protocols that have been suggested in the past that rely upon ground state cooling.

Acknowledgements– We thank Albert Schliesser, Eugene Polzik, Kartik Srinivasan, John Lawall and Anders Sorensen for helpful discussions. Funding is provided by DARPA QuASAR and the NSF Physics Frontier at the JQI.

[1] T. J. Kippenberg and K. J. Vahala, Science **321**, 1172 (2008).

[2] M. Aspelmeyer, T. J. Kippenberg, and F. Marquardt, Rev. Mod. Phys. **86**, 1391 (2014).

[3] J. Chan, T. P. M. Alegre, A. H. Safavi-Naeini, J. T. Hill, A. Krause, S. Gröblacher, M. Aspelmeyer, and O. Painter, Nature **478**, 89 (2011).

[4] T. P. Purdy, P.-L. Yu, R. W. Peterson, N. S. Kampel, and C. A. Regal, Phys. Rev. X **3**, 031012 (2013).

[5] A. H. Safavi-Naeini, S. Groblacher, J. T. Hill, J. Chan, M. Aspelmeyer, and O. Painter, Nature **500**, 185 (2013).

[6] A. Nunnenkamp, K. Børkje, and S. M. Girvin, Phys. Rev. Lett. **107**, 063602 (2011).

[7] P. Rabl, Phys. Rev. Lett. **107**, 063601 (2011).

[8] A. Kronwald and F. Marquardt, Phys. Rev. Lett. **111**, 133601 (2013).

[9] M.-A. Lemonde, N. Didier, and A. A. Clerk, Phys. Rev. Lett. **111**, 053602 (2013).

[10] K. Børkje, A. Nunnenkamp, J. D. Teufel, and S. M. Girvin, Phys. Rev. Lett. **111**, 053603 (2013).

[11] X. Xu, M. Gullans, and J. M. Taylor, Phys. Rev. A **91**, 013818 (2015).

[12] X. Xu and J. M. Taylor, Phys. Rev. A **90**, 043848 (2014).

[13] P.-L. Yu, K. Cicak, N. S. Kampel, Y. Tsaturyan, T. P. Purdy, R. W. Simmonds, and C. A. Regal, Applied Physics Letters **104**, 023510 (2014), http://dx.doi.org/10.1063/1.4862031.

[14] A. H. Safavi-Naeini, J. T. Hill, S. Meenehan, J. Chan, S. Gröblacher, and O. Painter, Phys. Rev. Lett. **112**, 153603 (2014).

[15] J. Gomis-Bresco, D. Navarro-Urrios, M. Oudich, S. El-Jallal, A. Griol, D. Puerto, E. Chavez, Y. Pennec, B. Djafari-Rouhani, F. Alzina, A. Martnez, and C. S. Torres, Nat Commun **5**, 4452 (2014).

[16] D. J. Larson, J. C. Bergquist, J. J. Bollinger, W. M. Itano, and D. J. Wineland, Phys. Rev. Lett. **57**, 70 (1986).

[17] C. J. Myatt, E. A. Burt, R. W. Ghrist, E. A. Cornell, and C. E. Wieman, Phys. Rev. Lett. **78**, 586 (1997).

[18] A. Jöckel, A. Faber, T. Kampschulte, M. Korppi, M. T.

Rakher, and P. Treutlein, Nat Nano **10**, 55 (2015).
[19] T. Ojanen and K. Børkje, Phys. Rev. A **90**, 013824 (2014).
[20] K. Stannigel, P. Rabl, A. S. Sørensen, P. Zoller, and M. D. Lukin, Phys. Rev. Lett. **105**, 220501 (2010).
[21] F. Marquardt, J. P. Chen, A. A. Clerk, and S. M. Girvin, Phys. Rev. Lett. **99**, 093902 (2007).
[22] H. Ooe, T. Sakuishi, M. Nogami, M. Tomitori, and T. Arai, Applied Physics Letters **105** (2014), 10.1063/1.4891882.
[23] A. Castellanos-Gomez, N. Agrat, and G. Rubio-Bollinger, Nanotechnology **20**, 215502 (2009).
[24] G. Ctistis, E. H. Frater, S. R. Huisman, J. P. Korterik, J. L. Herek, W. L. Vos, and P. W. H. Pinkse, Journal of Physics D: Applied Physics **44**, 375502 (2011), arXiv:1103.5892.
[25] J. Chan, M. Eichenfield, R. Camacho, and O. Painter, Opt. Express **17**, 3802 (2009).
[26] S. Joshi, S. Hung, and S. Vengallatore, EPJ Techniques and Instrumentation **1**, 1 (2014).
[27] K. Y. Yasumura, T. D. Stowe, E. M. Chow, T. Pfafman, T. W. Kenny, B. C. Stipe, and D. Rugar, Journal of Microelectromechanical Systems **9**, 117 (2000).
[28] Z. Hao, A. Erbil, and F. Ayazi, Sensors and Actuators A: Physical **109**, 156 (2003).
[29] S. A. Chandorkar, M. Agarwal, R. Melamud, R. N. Candler, K. E. Goodson, and T. W. Kenny, in *Micro Electro Mechanical Systems, 2008. MEMS 2008. IEEE 21st International Conference on Micro Electro Mechanical Systems* (2008) pp. 74–77.
[30] J. H. Ko, J. Jeong, J. Choi, and M. Cho, Applied Physics Letters **98**, 171909 (2011), http://dx.doi.org/10.1063/1.3575560.
[31] C. Zener, Phys. Rev. **53**, 90 (1938).
[32] V. T. Srikar and S. D. Senturia, Journal of Microelectromechanical Systems **11**, 499 (2002).
[33] R. Lifshitz and M. L. Roukes, Phys. Rev. B **61**, 5600 (2000).